

# Charged particle identification by the time-of-flight method in the BM@N experiment

K. Alishina<sup>1</sup>, V. Plotnikov<sup>1</sup>, L. Kovachev<sup>1,2</sup>, Yu. Petukhov<sup>1</sup>, M. Romyantsev<sup>1</sup>

*1 Joint Institute for Nuclear Research, Dubna, R -141980, Russia*

*2 Plovdiv University "Paisii Hilendarski", Plovdiv, 4000, Bulgaria*

*e – mail: [alishinaks@yandex.ru](mailto:alishinaks@yandex.ru)*

## Abstract

Baryonic Matter at Nuclotron (BM@N) is a fixed target experiment at the NICA – Nuclotron accelerator complex (JINR). It is aimed at studies of high-density nuclear matter in nuclear-nuclear (up to gold-gold) collisions. This paper focuses on identification of light charge particles ( $\pi$ , K, p) and fragments ( $\text{He}^3$ , d/ $\text{He}^4$ , t) in the BM@N experiment using the time-of-flight method. For now, the method allows separating the light particles up to 2 GeV/c and the light fragments up to 4 GeV/c.

## Идентификация заряженных частиц времяпролетным методом на эксперименте BM@N

К. Алишина<sup>1</sup>, В. Плотников<sup>1</sup>, Л. Ковачев<sup>1,2</sup>, Ю. Петухов<sup>1</sup>, М. Румянцев<sup>1</sup>

*1 Объединенный институт ядерных исследований, Дубна, 141980, Россия*

*2 Пловдивский университет им. "Паусия Хилендарского", Пловдив, 4000, Болгария*

*e – mail: [alishinaks@yandex.ru](mailto:alishinaks@yandex.ru)*

## Аннотация

Барионная материя на нуклотроне (BM @N) - эксперимент с фиксированной мишенью на ускорительном комплексе NICA - Нуклотрон (ОИЯИ). Он направлен на изучение ядерной материи высокой плотности в ядерно-ядерных (вплоть до Au-Au) столкновениях. Эта статья посвящена идентификации частиц легкого заряда ( $\pi$ , K, p) и фрагментов ( $\text{He}^3$ , d/ $\text{He}^4$ , t) в эксперименте BM@N с использованием времяпролетного метода. На данный момент метод позволяет разделять легкие частицы до 2 ГэВ/с и легкие фрагменты до 4 ГэВ/с.

## Introduction

Relativistic heavy ion collisions provide the unique opportunity to study nuclear matter under extreme density and temperature. In the collision, nuclear matter is heated up and compressed for a very short period of time. At moderate temperatures, nucleons are excited to baryonic resonances which decay by the emission of mesons. At higher temperatures, also baryon-antibaryon pairs are created. This mixture of baryons, antibaryons and mesons, all strongly interacting particles, is denoted as hadronic matter or baryonic matter if baryons dominate [1,2].

32           The study of strange particle production in nucleus-nucleus interactions within the beam  
33 energy range of 2 – 3.8 GeV per nucleon is one of the main goals of the BM@N experiment at the  
34 Nuclotron accelerator [3,4]. To detect charged particles and nucleus fragments, an identification  
35 system is needed. The time-of-flight detectors TOF-400 and TOF-700 are used for this purpose. The  
36 particle momentum measured in the tracking detectors and the time-of-flight data determines the  
37 mass of charged particles. In the previous stage of the analysis, the measured time information was  
38 corrected to the amplitude of signals dependence (slewing correction), as well as aligned to the  
39 absolute scale for each TOF channel.

40           As a result of the current work, an algorithm for identifying charged particles was developed  
41 and applied to experimental data. Realistic Monte Carlo (MC) simulation was constructed. The  
42 efficiency of each detector subsystem used for the particle identification was determined.

## 43 **2 Experimental set-up**

44           The experimental run of the BM@N detector was performed with the Ar/Kr beam in March  
45 2018. The view of the BM@N set-up used in the run is presented in Fig. 1. The experimental data  
46 from the central tracker, outer cathode strip chamber (CSC) [5], drift chambers (DCH), time-of-  
47 flight detectors (TOF), zero-degree calorimeter (ZDC), trigger and T0 detectors (T0T) were read out  
48 using the integrated data acquisition system.

49           The CSC is a two-coordinate detector with the cathode readout. It is used for the first time in  
50 this dataset session. The CSC is used as a filter for bad tracks. The DCH consists of four double  
51 coordinate planes and also used as a filter for bad tracks. Another purpose of the DCH is measuring  
52 the angular distribution and momentum of the beam. The configuration of the central tracker (CT)  
53 was based on three planes of the forward silicon detector (Si) with double-side readout and six two-  
54 coordinate GEM (Gaseous Electron Multiplier) stations combined from six GEM detectors. The  
55 GEM stations are placed inside the analyzing magnet in such a way that electron drift direction is  
56 opposite from station to station. It was done to avoid a systematic shift of reconstructed hits due to  
57 the Lorentz force in the magnetic field  $\sim 0.6$  T. The Lorentz shift varies from 0.9 to 1.5 mm for  
58 GEM stations.

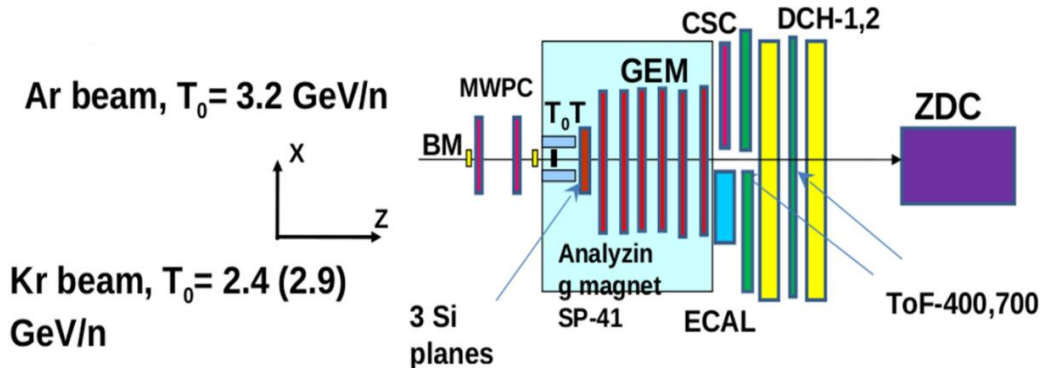


Fig.1. Scheme of the experimental set-up.

Time-of-flight detectors are included in the set-up for particle identification. TOF-400 and TOF-700 detectors based on multi-gap resistive chambers (mRPC) with a strip readout allow us to discriminate hadrons ( $\pi$ ,  $K$ ,  $p$ ) as well as light nuclei with the momentum up to few GeV/c. The starting time of passage of the particles is recorded by the starting counter  $T_0$ .

### 3 Identification procedure

In this section, we describe the identification procedure for the experimental data analysis.

A TOF particle identification system is needed to determine the type (mass) of charged particles and nuclear fragments. For this, it is necessary to measure the time of flight and track length for calculation of the particle velocity. For the time measurements, we use TDC with 25 ps time bin [6] and take into account nonlinear corrections. At the first stage, the responses of all channels of the time-of-flight system (and also the  $T_0$  time response) were corrected to the amplitude dependence (slewing corrections) and also aligned in time. And the procedure of absolute calibration of the time of flight of particles to the TOF detectors was also carried out using the data on the passage length and time of protons with a known momentum.

At the present stage, we made an alignment of subdetectors in two identification chains (subdetector chains): CT–CSC–TOF-400 and CT–DCH–TOF-700. We used events without magnetic field for the alignment purposes. The outer trackers and TOF detectors are aligned by using straight GEM tracks applying only the X, Y, Z shifts and with a rotation around the Z axis in some cases.

We developed an algorithm to identify types of charged particles and nuclear fragments required for physical analysis based on the calibrated time signals from the TOF-400 and TOF-700 detectors and the track momenta measured in the central tracker detectors and extrapolated to the TOF detectors using outer tracking detectors (CSC or DCH) of the BM@N set-up. We use events where a primary vertex (PV) was reconstructed with at least two tracks. We extrapolate the track we want to identify to the Z-plane of the PV and calculate the X and Y distances to the PV. We reject

86 the tracks which are out of a distance of more than 1 cm from the PV. We also reject the tracks with  
 87 less than five hits in the central tracker. The track reconstructed in the central tracker is extrapolated  
 88 to the Z coordinate of the outer detector (CSC or DCH) and is matched with nearest hit in the outer  
 89 detector within a predefined distance. The value of this distance is determined usually as  $3\sigma$  of the  
 90 Gaussian fit of the distribution of the deviation between hits and tracks. If the track is matched in  
 91 the outer tracker, we extrapolate it to the TOF detector (TOF-400 or TOF-700). The matching  
 92 procedure for the TOF detector is almost the same as for the matching central track with the outer  
 93 tracker. An appropriate fixed cut is used in each case for the distance between the TOF hit and track  
 94 crossing point.

95 The particle identification is carried out using the TOF-400 and TOF-700 detectors  
 96 separately. In the future, both approaches are planned to be combined. The particle identification  
 97 using time-of-flight measurements requires good time resolution. The presently achieved time  
 98 resolution for the TOF-400 detector is about  $\Delta t$  84ps (see Fig.2) and for the TOF-700 detector is  
 99 about  $\Delta t$  115ps.

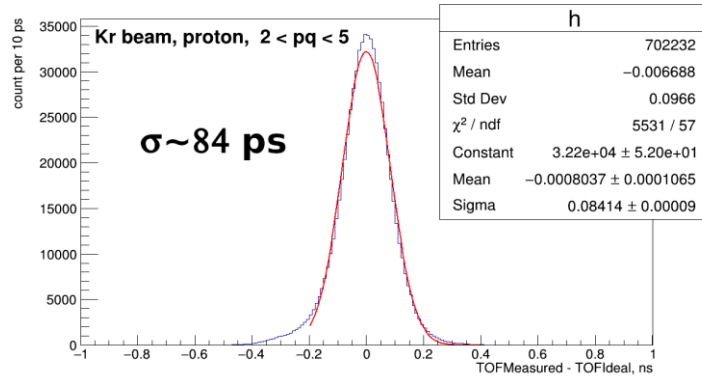


Fig.2. TOF-400 time resolution.

100  
101

102 Charged particle identification was performed using the time-of-flight method. The formula  
 103 for determining the mass of a particle has a form:

$$104 \quad m = p \sqrt{\frac{1}{\beta^2} - 1}, \beta = \frac{L}{ct}, \quad (1)$$

105 where  $m$  – mass of the particle,  $p$  – momentum of the particle,  $L$  – length of the particle track,  
 106  $c$  – speed of light,  $t$  – time of flight,  $\beta$  – speed of the particle in units of the speed of light. The mass  
 107 squared resolution can be determined by the following formula:

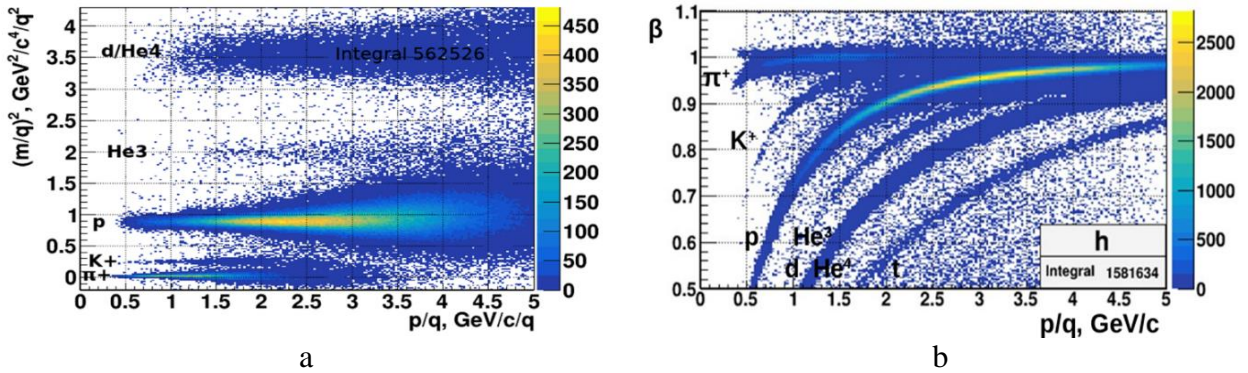
$$108 \quad \frac{dm^2}{m^2} = \sqrt{\left(\frac{2dp}{p}\right)^2 + \left(\frac{2}{1-\beta^2}\right)^2 \left(\frac{dt}{t}\right)^2 + \left(\frac{2}{1-\beta^2}\right)^2 \left(\frac{dL}{L}\right)^2} \quad (2)$$

109 For the low momentum, the mass squared uncertainty is determined by the particle  
 110 momentum uncertainty, and for the high momentum, it is determined by the time of flight due to the

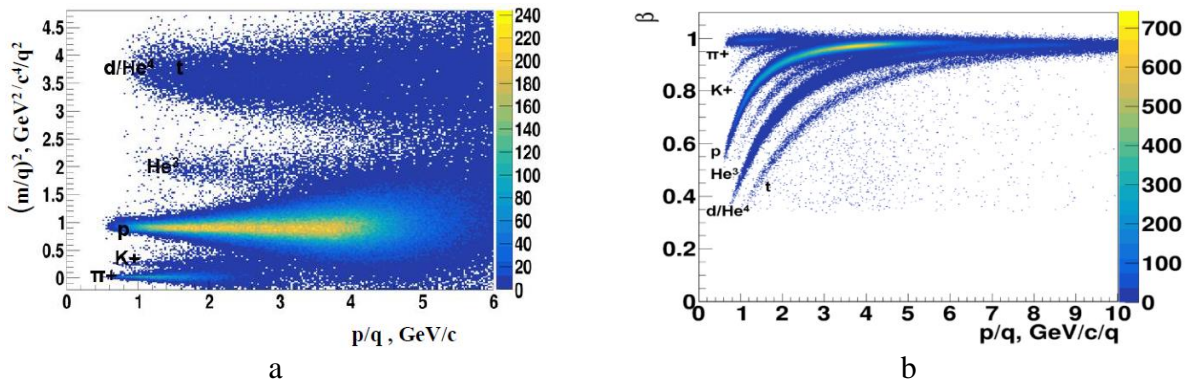
111 Lorentz factor. The relative uncertainty of the track length is few times less than the relative  
 112 uncertainty of the time, so we can neglect it.

#### 113 4 First identification results from the data

114 The first results of identification of light charged particles ( $\pi$ , K, p) and nuclear fragments  
 115 (He3, d / He4, t) were obtained using the TOF-400 and TOF-700. Identification is performed in  
 116 inelastic reactions  $\text{Ar} + \text{A} \rightarrow \text{X}$  with the kinetic energy of the argon beam of 3.2 AGeV and various  
 117 targets (C, Al, Cu, Sn, Pb). Fig. 3a and 4a show the calculated particle mass squares as a function of  
 118 the particle momentum. The speed of a particle in the units of the speed of light is shown as a function  
 119 of momentum in Fig. 3b and 4b. The distributions of the squared mass and velocity  $\beta$  as functions  
 120 of momentum show that the spectra of particles and nuclear fragments are well separated



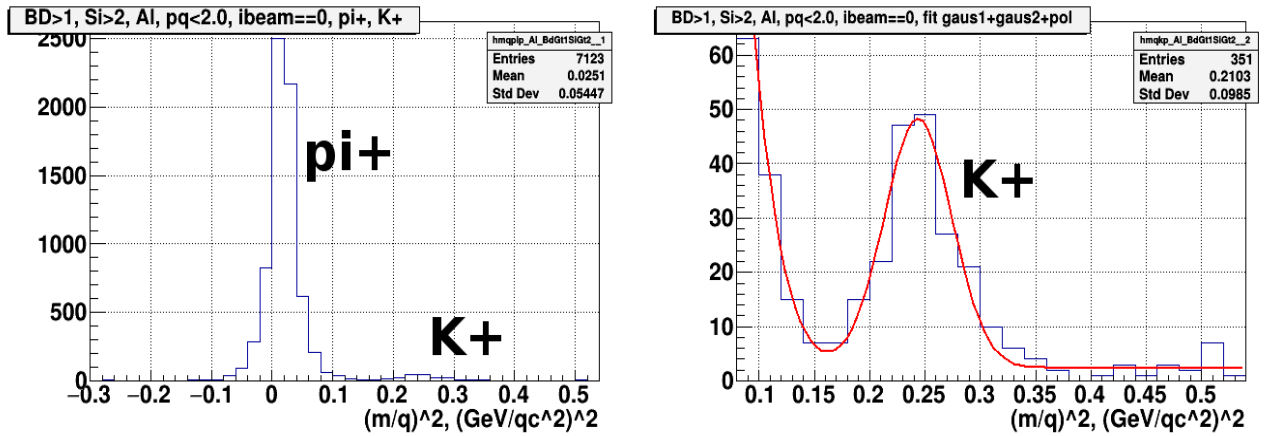
121 Fig.3. a) The square of the mass-to-charge ratio  $(m/q)^2$  as a function of the momentum-to-charge  
 122 ratio  $p/q$  of positively charged particles, measured in the TOF-400 system. Identified  $\pi^+$ ,  $K^+$ , p,  
 123 He3, d/He4 are visible as populated bands of particles; b) Velocity  $\beta = v/c$  as a function of the  
 124 momentum-to-charge ratio  $p/q$  of positively charged particles, measured in the TOF-400 system.  
 125 Identified  $\pi^+$ ,  $K^+$ , p, He3, d/He4, t are visible as populated bands of particles.



126 Fig.4. a) The square of the mass-to-charge ratio  $(m/q)^2$  as a function of the momentum-to-charge  
 127 ratio  $p/q$  of positively charged particles, measured in the TOF-700 system. Identified  $\pi^+$ ,  $K^+$ , p,  
 128 He3, d/He4 are visible as populated bands of particles; b) Velocity  $\beta = v/c$  as a function of the  
 129 momentum-to-charge ratio  $p/q$  of positively charged particles, measured in the TOF-700 system.  
 130 Identified  $\pi^+$ ,  $K^+$ , p, He3, d/He4, t are visible as populated bands of particles.

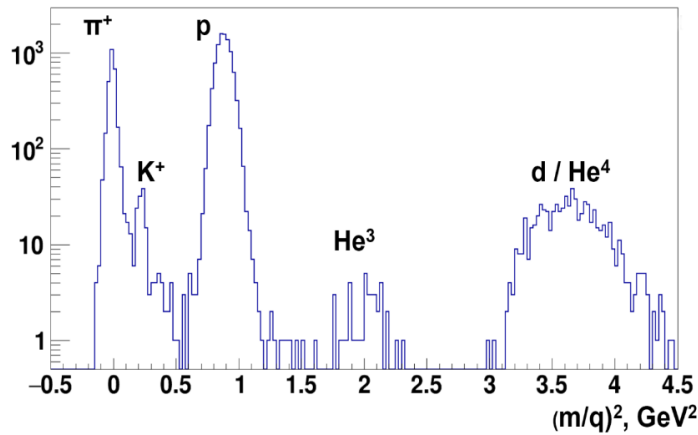
131 Using formula (2) and the proton band width from Fig.3a, we determined the relative  
 132 uncertainty of the identified track momentum. It is close to 2.5 % in the momentum range we plan  
 133 to study in future analysis, and is almost constant.

134 The squared mass distribution is used to extract the number of  $K^+$  and  $\pi^+$ . About  $2 \cdot 10^3$   $K^+$   
 135 and  $10^5$   $\pi^+$  were identified in the Ar data for the CT–CSC–TOF-400 subdetector chain. Fig. 5a and  
 136 5b show that a good separation of  $K^+$  and  $\pi^+$  was obtained.



137  
 138

a

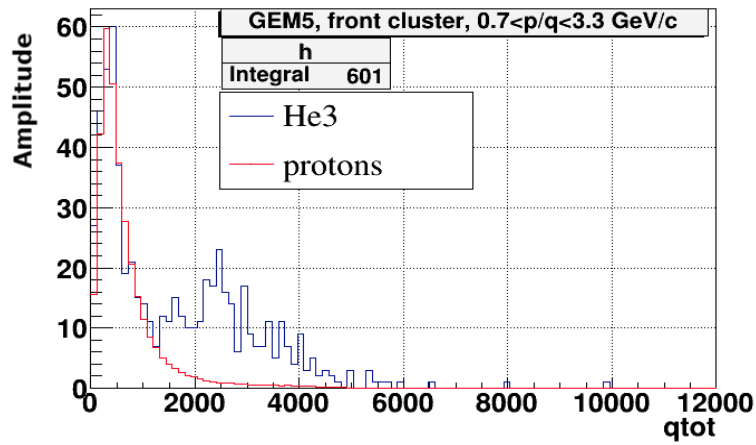


139  
 140

b

141 Fig.5. a) Distribution of the square of the mass-to-charge ratio of particles identified in the TOF-  
 142 400 system; b) Distribution of the square of the mass-to-charge ratio of particles identified in the  
 143 TOF-700 system.

144  $He^3$  can be separated from the background with atomic number  $Z=1$  using the amplitudes of  
 145 the clusters in the GEMs. This is clearly seen from Fig. 6. The same technique can be used to separate  
 146  $He^4$  from d in future analysis.



147

148 Fig.6. Amplitude of the GEM5 cluster signal from the identified tracks, He<sup>3</sup> and proton bands.

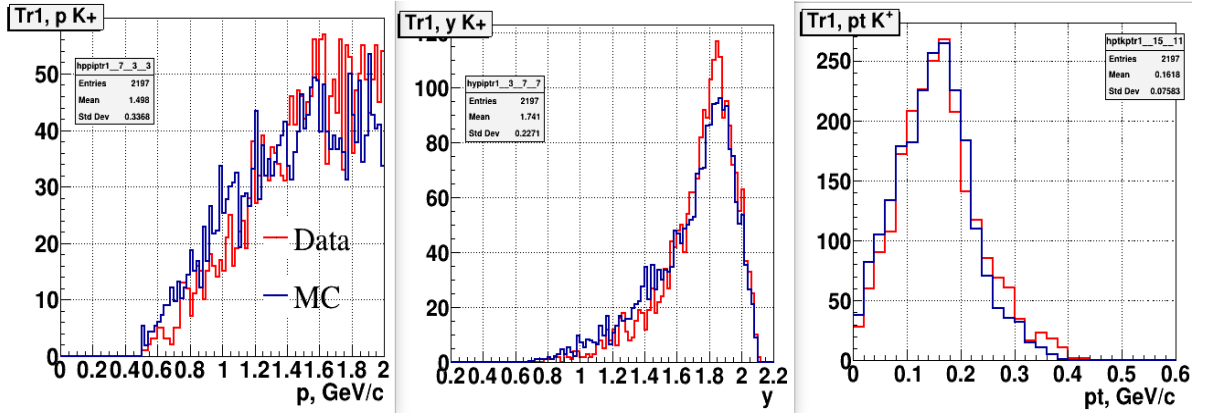
## 149 5. Simulation

150 We have implemented a realistic MC simulation with all detectors used in identification. We  
 151 used a minimum bias UrQMD generator that produces particles during the collision of heavy ions.  
 152 Some realistic detector effects for the central tracker were implemented to the MC in the previous  
 153 stage of the analysis. It is the evolution of an electron avalanche in a magnetic field in GEM  
 154 detectors, realistic strip signals in Si and GEM detectors. At this stage of the analysis, we have  
 155 implemented real Lorenz shifts to the MC, normalized the Si, GEM and CSC signals in the MC on  
 156 the data, adjusted the MC CSC cluster width to the data, and smeared MC hits for Si and GEM to  
 157 obtain the same residuals in the MC as in the data. For the MC, the same identification procedure is  
 158 implemented as for the data, except for the calibration and alignment of the detectors. We have  
 159 implemented the same geometry for CT, CSC and TOF-400 for MC that we got from the data.

160 We also have determined the efficiency for each detector used in the identification procedure,  
 161 taking into account the results of modeling and reconstruction of nucleus-nucleus interactions. For  
 162 Si and GEM stations, the average efficiency ranges from 80 to 95 %. For the CSC, the average  
 163 efficiency also ranges from 80 to 95 % except for the top left corner of the CSC with broken readout  
 164 electronics. For TOF-400, the average efficiency varies from 65 to 80% for different planes. For  
 165 TOF-700, it is 80 90 % for different planes, with the exception of a few broken planes.

166 We have implemented detector efficiencies for CT, CSC and TOF-400 in the MC.  
 167 Verification of the MC efficiency calculation shows agreement with the efficiencies that we obtained  
 168 for these detectors from the data (better than 5 %).

169 A comparison of the raw K<sup>+</sup> spectra of the total momentum, rapidity and transverse  
 170 momentum for the MC with all implemented realistic effects and detector efficiencies with  
 171 experimental data is shown in Fig.7. There is good agreement.



172

173 Fig.7. Spectra of total momentum  $p$ , rapidity  $y$ , transverse momentum  $pt$   $K^+$  for MC and data.

## 174 Summary and plans

175 Good quality charged particles identification was obtained and the tiny  $K^+$  signal was  
 176 separated from the large  $\pi^+$  contribution.

177 The test CSC outer tracker shows good usability. The CSC assembly technique is approved.  
 178 The CSC detector description is implemented into the reconstruction chain of the BM@N  
 179 experiment. The tracks from the central tracker were refined using the CSC and matched to the TOF-  
 180 400 hits. During the analysis, the TOF-400 calibration was improved and the good time resolution  
 181 ( $\Delta t = 84ps$ ) was achieved. The good performance of the CSC motivates their extended usage in the  
 182 next run.

183 The matching of the central tracker, outer DCH tracker and TOF-700 has been successfully  
 184 completed. During the analysis, the good time resolution of  $\Delta t 115ps$  for TOF-700 was achieved.

185 The realistic MC with basic detector effects and efficiencies was implemented for the CT-  
 186 CSC-TOF-400 subdetector chain. Good agreement is observed for  $K^+$ . We plan to implement a  
 187 realistic MC for the CT-DCH-TOF-700 subdetector chain following the same procedure. We also  
 188 need to improve our MC to describe  $\pi^+$  distributions.

189 In the future work, we plan to extract the yields of charged particles. The measurement of  
 190 the dependence of the yields of charged strange mesons on the collision energy of nuclei near and  
 191 below the production threshold is a tool for determining the compressibility of nuclear matter  
 192 described by the equation of state.

## 193 Acknowledgements

194 We acknowledge the support of the RFBR grant No 18 – 02 – 40036 and we are thankful to  
 195 the working group of BM@N.



196 **References**

197 [1] J. Adams et al, Nucl. Phys. A 757, 102-183 (2005)

198 [2] K. Adcox et al, Nucl. Phys. A 757, 184-283 (2005)

199 [3] BM@N Conceptual Design Report. [http://nica.jinr.ru/files/BM@N/BMN\\_CDR.pdf](http://nica.jinr.ru/files/BM@N/BMN_CDR.pdf)

200 [4] M. Kapishin (for the BM@N Collaboration), Nucl.Phys. A982 (2019) 967-970.

201 [5] A. Galavanov et al 2020 JINST15 C09038.

202 [6] <http://afi.jinr.ru/TDC64V>